American Mineralogist, Volume 76, pages 1722–1727, 1991

Brushite, hydroxylapatite, and taranakite from Apulian caves (southern Italy): New mineralogical data

SAVERIO FIORE
Istituto di Ricerca sulle Argille, C.N.R., Via Nazario Sauro, 85, 85100 Potenza, Italy
ROCCO LAVIANO
Dipartimento Geomineralogico, Università degli Studi di Bari, Campus Universitario, 70124 Bari, Italy

ABSTRACT

Samples of brushite, hydroxylapatite, and taranakite collected from seven karst caves of Apulia (southern Italy) have been investigated by means of chemical analysis and by DTA and XRD techniques. Brushite is found to crystallize in very pure form, whereas hydroxylapatite and taranakite show several isomorphous substitutions. A high Zn content was detected in hydroxylapatite. The TG curves for one sample of hydroxylapatite show a weight loss greater than the total H_2O content, probably because of the loss of S. DTA and XRD analyses of taranakite indicate that the formation of $AlPO_4$ at 1200 °C is not a reversible reaction.

In accord with previously published paragenetic sequences, the minerals were probably formed by interaction between phosphatic solutions derived from bat guano and the substratum minerals, specifically calcite and clay minerals. However, the data also suggest precipitation from solution for brushite and hydroxylapatite.

INTRODUCTION

Little has been reported (Murray and Dietrich, 1956; Balenzano et al., 1974; Sakae and Sudo, 1975) concerning the mineralogical properties of brushite, hydroxylapatite, and taranakite associated with bat guano deposits from caves because they occur rarely and sampling is difficult. In this study, several samples collected from seven Apulian karst caves (southern Italy) are analyzed.

MODE OF OCCURRENCE AND EXPERIMENTAL METHODS

The sampled caves are in a Cretaceous limestone that constitutes the Apulian Platform (southern Italy). The caves were selected because they were accessible and appreciable amounts of bat guano were present. The location of the caves, their description, and identification code number are reported by Orofino (1965). All the caves have high humidity and a large amount of damp bat guano; only cave PU 1211 presents a comparatively small mass of guano.

Brushite (hereafter BR) occurs as a continuous pastelike layer up to 20 cm thick between guano and limestone or as very small pulverulent masses irregulary distributed throughout the guano. Hydroxylapatite (hereafter HAP) is frequently found as small grains (0.5–1.5 mm) within the brushite layer and rarely as thin crusts on calcitic concretions that underlie the guano. BR is always more abundant than HAP, except in cave PU 1211 where we have found the inverse relation. Taranakite (hereafter TR) forms irregular aggregates within the insoluble residuum of limestone ("terra rossa") and also occurs within the guano as fine layers (2–3 mm thick) parallel to the calcareous substratum. In some caves, other phosphates such as ardealite, francoanellite, strengite, variscite, and vivianite are present, as shown by X-ray powder diffraction patterns.

The samples for analysis were separated and purified under a binocular microscope by hand picking, and the grains were then cleaned by a weak ultrasonic treatment. Refractive indices were determined in calibrated oils (estimated error = ±0.002). X-ray analyses were performed using a Philips powder diffractometer (PW 1710) with Ni-filtered Cu$K\alpha$ radiation and 0.01° 2θ step scans. Counting time was 30 s per step, and a NaF internal standard was employed. X-ray powder diffraction patterns of previously heated samples were recorded at room temperature. Cell parameters were refined by the least-squares method. Chemical analyses were obtained using an X-ray fluorescence spectrometer (Philips PW 1410) for major elements and atomic absorption spectrophotometry (Perkin Elmer 5100) for minor and trace elements. H_2O was measured using the Penfield method. DTA and TG curves were obtained using a Netzsch simultaneous thermal apparatus (STA 409) under the following working conditions: thermocouples, Pt-Pt/Rh; reference, Al_2O_3; heating rate, 5 °C per min; DTA sensitivity, 100 μV; TG sensitivity, 25–50 mg; sample weight, 50–100 mg; static air atmosphere.

RESULTS

Brushite

Brushite, $CaHPO_4 \cdot 2H_2O$, forms cryptocrystalline pastelike aggregates varying in color from white-ivory to yellow-ivory; in cave PU 32 only it occurs as colorless

0003–004X/91/0910–1722$02.00

platey crystals 0.6–0.8 mm in size. The mineral is optically biaxial with refractive indices and $2V$ values that fall within narrow ranges. In the several samples examined, values of $\alpha = 1.540$, $\beta = 1.546$, $\gamma = 1.552$, and $2V \approx 90°$ have been frequently observed. This homogeneity is related to the extreme chemical purity of the mineral. Six samples collected from different caves have given the following mean values (wt% $\pm \sigma$): CaO = 33.12 ± 0.98, P_2O_5 = 40.53 ± 0.87, H_2O = 26.19 ± 0.31; only Fe, Zn, and S are present as trace elements (<100 ppm).

The X-ray powder diffraction patterns, indexed on a monoclinic cell with space group $C2/c$ (PDF 9-77), demonstrate that the samples are well crystallized and have very similar d-values. The differences between the unit-cell parameters of the seven samples investigated are very slight, with mean values: $a = 6.361(3)$, $b = 15.191(4)$, $c = 5.814(2)$, $\beta = 118.45(4)$.

In accord with previous authors (Murray and Dietrich, 1956; Balenzano et al., 1974), the DTA curves shows two endothermic peaks (195 °C and 410 °C) from the reactions $CaHPO_4 \cdot 2H_2O \rightarrow CaHPO_4$ (monetite) + $\uparrow 2H_2O$ and $2CaHPO_4 \rightarrow Ca_2P_2O_7$ (amorphous) + $\uparrow H_2O$, with weight losses of 21% and 25%, respectively; the exothermic peak (at 495 °C) results from the transformation $Ca_2P_2O_7$ (amorphous) → $Ca_2P_2O_7$ (crystalline). Only slight differences in temperature (±15 °C) and peak sharpness were recorded among the different samples.

Hydroxylapatite

Hydroxylapatite [$Ca_5(PO_4)_3OH$] always appears as small yellowish or brown grains ranging from 0.5 to 1.5 mm in size. Although these grains are frequently included within the BR masses, an intimate association between the two minerals never has been observed. The mineral generally forms yellow-brown lumps or occasionally pale yellow plates that are uniaxial negative and display weak pleochroism. The refractive index values, measured only on two samples because the crystals are too small to provide reliable data, are $\omega = 1.651$ and $\epsilon = 1.645$ for sample PU 502/3, $\omega = 1.638$ and $\epsilon = 1.628$ for sample PU 1211/2. X-ray powder diffraction patterns of the samples (Table 1) exhibit very different d-values. Indeed, the crystallinity index (CI), calculated as suggested by Simpson (1964), indicates a continuous variation from low (CI = 0.10 for PU 71/5) to very high crystallinity (CI = 0.03 for PU 1211/2) (Table 1). Although the a and c values vary from one specimen to another, the c/a ratio (Table 1) is almost constant and close to those of hydroxyl-bearing varieties of apatite (Deer et al., 1965).

The Apulian HAP shows limited substitution of Mg, Zn, Na, and K for Ca and S for P. Moreover, all the samples contain Sr (25–134 ppm), Cu (217–575 ppm), Mn (346–867 ppm), and Cl (35–54 ppm) as trace elements. It is interesting to note the relatively high Zn content (>0.55% ZnO), which, in accordance with Balenzano et al. (1974), seems a typical feature of samples from Apulian caves.

Tracings of the DTA and TG curves of HAP are given in Figure 1. The DTA curve shows only a broad exothermic effect between 1100 and 1200 °C, whereas the TG curve gradually declines. On the basis of powder diffraction patterns of the products heated at 1000 and 1400 °C, we suggest the following reactions:

$$2[Ca_5(PO_4)_3OH] \rightarrow 2[\beta\text{-}Ca_3(PO_4)_2] \text{ (whitlockite)} + Ca_4P_2O_9 + \uparrow H_2O \text{ (1000 °C)}$$

$$\beta\text{-}Ca_3(PO_4)_2 \rightarrow \alpha\text{-}Ca_3(PO_4)_2 \text{ (1400 °C)}.$$

A greater weight loss has been recorded for sample PU 1211/2, probably because of released SO_3.

Taranakite

At present, the structure of TR is unknown, even though several studies have been carried out on both natural and synthetic products (Haseman et al., 1950, 1951; Murray and Dietrich, 1956; Smith and Brown, 1959; Balenzano et al., 1974; Sakae and Sudo, 1975; Filipov, 1978a). The chemical formula most frequently adopted is $H_6K_3Al_5(PO_4)_8 \cdot 18H_2O$, as given by Smith and Brown (1959) who also proposed a hexagonal six-layer structure with $a = 8.71$ Å, $c = 96.1$ Å, and $Z = 6$. McConnell (1976) suggested that TR could be considered to be a phyllophosphate rather than orthophosphate; he proposed a hexagonal structure, with $a = 8.71$ Å and $c = 96.1$ Å, composed of six double layers of $4[(X_4O_{10})(OH)_2]$, where X = P, Al, or (H_3). McConnell assigned the chemical formula $K_x[Al_{2-y}(H_3)_y](OH)_2[Al_xP_{4-x-z}(H_3)_zO_{10}]$ to TR in analogy to that of illite, which is one of the reactants from which TR can be formed. However, Fleischer (1987) reports the formula $KAl_3(PO_4)_3OH \cdot 9H_2O$ but assigns francoanellite (Balenzano et al., 1976), a mineral structurally related to TR, the formula $H_6K_3Al_5(PO_4)_8 \cdot 13H_2O$. Because there is no well-established structure of the mineral and in consideration of our data, we have decided to adopt the suggestion of Smith and Brown (1959) so as not to create further confusion and to preserve the analogies between the formulae of TR and francoanellite.

The aggregates of TR from Apulian caves form as yellowish white, claylike, soft nodular masses. Under the microscope, the mineral appears as a fine-grained powder and rarely as pseudohexagonal, thin colorless plates that are uniaxially negative. Several determinations of refrac-

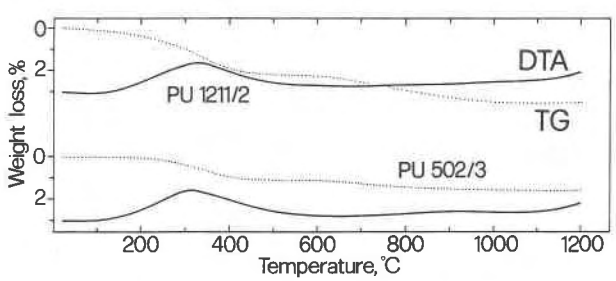

Fig. 1. DTA and TG curves of hydroxylapatite.

TABLE 1. Hydroxylapatite: Data from X-ray powder diffraction patterns, cell parameters, and formulas

	PU 71/5		PU 394/2		PU 502/3		PU 1211/2	
hkl	*d*	I/I_0	*d*	I/I_0	*d*	I/I_0	*d*	I/I_0
100	8.19	14	8.13	9	8.15 b	10	8.18	15
101	—	—	5.28	5	5.26	6	5.25	2
110	4.73	4	—	—	—	—	4.73	2
200	—	—	4.05	5	4.07 b	2	4.08	7
111	3.90	10	3.89	17	4.02 b	2	3.88	8
201	—	—	3.50 b	1	—	—	3.50	4
002	3.43	51	3.43	43	3.44	43	3.44	44
102	3.17 b	10	3.16 b	17	3.16 b	4	3.16	9
210	3.09	16	3.07	32	3.08 b	13	3.09	16
211	2.821	100	2.812	100	2.825	100	2.811	100
112	2.787	93	2.778	76	2.789	100	2.779	68
300	2.727	50	2.724	55	2.736	63	2.717	60
202	2.635	24	2.629	22	2.633	21	2.628	26
301	2.541	6	—	—	2.529 b	6	2.531	5
212	2.300 b	12	2.295	12	2.302 b	9	2.292	7
310	2.272	24	2.266	20	2.268 b	17	2.261	18
221	2.234	6	2.224	2	—	—	2.231	3
311	2.157	4	2.146	7	2.148	8	2.145	6
302	2.137	4	—	—	—	—	2.129	3
113	2.066	4	—	—	2.061	6	2.058	5
400	2.043	4	2.042	2	—	—	2.042	1
203	1.996	5	—	—	2.000	6	1.993	4
222	1.948	20	1.945	25	1.948	22	1.941	24
312	1.891 b	8	1.891	12	1.893	10	1.887	10
320	1.871	6	1.872	3	1.877	6	1.868	4
213	1.839	33	1.841	30	1.845	27	1.839	30
321	—	—	1.807	22	1.809	6	1.803	12
410	1.786 b	9	1.781	7	1.782	6	1.778	10
402	1.753 b	8	1.755	6	1.759	8	1.753	10
004	1.718	19	1.721	25	1.723	17	1.719	13
104	—	—	1.686	4	—	—	1.681	3
322	—	—	1.646	6	—	—	1.644	4
a (Å)	9.458(6)		9.419(5)		9.448(6)		9.410(2)	
c (Å)	6.869(4)		6.883(4)		6.891(7)		6.876(2)	
c/*a*	0.726		0.731		0.729		0.731	
CI	0.10		0.08		0.09		0.03	
PU 71/5	$(Ca_{9.50}Mg_{0.04}Zn_{0.09}Na_{0.26}K_{0.03})(P_{5.82}S_{0.24})O_{24.12}(OH)_{1.88}$							
PU 394/2	$(Ca_{9.70}Mg_{0.04}Zn_{0.21}Na_{0.04}K_{0.01})(P_{5.97}S_{0.03})O_{23.94}(OH)_{2.06}$							
PU 502/3	$(Ca_{9.86}Mg_{0.04}Zn_{0.07}Na_{0.04}K_{0.01})(P_{5.97}S_{0.03})O_{24.00}(OH)_{2.00}$							
PU 1211/2	$(Ca_{9.67}Mg_{0.07}Zn_{0.07}Na_{0.09}K_{0.06})(P_{5.86}S_{0.15})O_{23.97}(OH)_{2.03}$							

Note: The formulas have been calculated on the basis of 26 (O,OH). CI: crystallinity index.

tive indices for different samples have shown values very close to $\omega = 1.508$, $\epsilon = 1.502$.

X-ray powder patterns of TR (Table 2) show sharp diffractions and a very strong (006) basal reflection. The values of *c* increase slightly with H_2O content (Table 2), and if one also takes into account the published data from Apulian TR (Balenzano et al., 1974), this tendency is more evident ($r = 0.809$ and $n = 7$, where r is the correlation coefficient and n is the number of samples). However, other values (Sakae and Sudo, 1975; Filipov, 1978a), do not fit this trend, and more data are needed to verify the relationship. The Apulian TR shows, as do almost all natural samples, very limited substitution of Ca and Na for K, Fe for Al, and S for P. Other elements, such as Rb, Cu, Mn, Sr, N, are present at <100 ppm.

The thermal data (Fig. 2) suggest that the two endothermic events at 80–140 °C and 140–300 °C (see also Balenzano et al., 1974; Sakae and Sudo, 1975) result from the reactions $H_6K_3Al_5(PO_4)_8 \cdot 18H_2O \rightarrow H_6K_3Al_5(PO_4)_8 \cdot 13H_2O + \uparrow 5H_2O$ and $H_6K_3Al_5(PO_4)_8 \cdot 13H_2O \rightarrow H_6K_3Al_5(PO_4)_8 + \uparrow 13H_2O$, respectively. X-ray diffraction patterns of the products heat-treated at 140 and 300 °C indicate that the former product is francoanellite, whereas the latter is noncrystalline. Between 300 and 500 °C, the product gradually loses more weight and is wholly dehydrated according to the reaction $H_6K_3Al_5(PO_4)_8 \rightarrow K_3Al_5P_8O_{29} + \uparrow 3H_2O$. The exothermic peak (565–595 °C) resulted from the crystallization of two new phases according to the reaction $K_3Al_5PO_8O_{29} \rightarrow 2AlPO_4 + 3KAlP_2O_7$. In agreement with Balenzano et al. (1974) the presence of $KAlP_2O_7$, a compound not reported in the JCPDS file, was assumed because the powder pattern of the product heat-treated at 620 °C contains the reflections of a compound similar to $KAl_{0.5}Fe_{0.5}P_2O_7$. Also, Sakae and Sudo (1975) reported a similar but uninterpreted powder pattern. A broad deflection is present on the DTA curves between 750 and 980 °C; it is more pronounced for samples PU 71/4 and PU 502/2, which also show a very slight weight loss. Such an endothermic effect was also recognized by Murray and Dietrich (1956) and by Sakae and Sudo (1975). The latter authors observed the disappearance of the three main reflections (5.72 Å, 2.94

TABLE 2. Taranakite: Data from X-ray powder diffraction patterns, cell parameters, and formulas

	PU 38/1		PU 71/3		PU 71/4		PU 71/6		PU 502/2	
hkl	*d*	I/I_0	*d*	I/I_0	*d*	I/I_0	*d*	I/I_0	*d*	I/I_0
006	15.82	100	15.57	100	15.89	100	15.60	100	16.01	100
0012	7.92	18	7.84	17	7.92	36	7.85	17	7.92	44
101	7.60	8	7.56 b	6	7.61	26	7.61	7	7.59	12
012	7.47	28	7.39	19	7.45	30	7.38	13	7.43	32
104	7.18	5	7.12 b	6	7.19	8	7.16	4	7.23	10
1010	5.91	17	5.87	7	5.91	13	5.86	8	5.92	24
0114	5.07	3	5.02	2	5.03	4	5.09	3	5.06	4
1016	4.67	4	4.63	3	4.67	4	4.63	3	4.68	5
110	4.35 b	12	4.33	10	4.35	12	4.32	7	4.36 b	18
113	4.32	18	4.29	12	4.32	17	4.31	8	4.33	20
1019	4.20	4	4.15 b	6	4.17 b	4	4.19	1	4.20	5
119	4.02 b	7	4.00 b	4	4.02	5	4.00	3	4.03	10
1112	3.82	40	3.80	12	3.82	24	3.81	17	3.81	35
202	3.75	11	3.73	8	3.75	10	3.73	5	3.75	13
208	3.59	22	3.57	8	3.59	12	3.57	9	3.60	22
0213	3.36	29	3.34	8	3.36	10	3.33	14	3.37	14
2014	3.30	14	3.29	7	3.30	9	3.28	5	3.30	14
0216	3.19	15	3.17	7	3.16	13	3.16	5	3.18	14
2017	3.14	31	3.13	12	3.14	22	3.13	15	3.14	35
0129	3.03 b	2	3.03	5	3.05 b	4	3.06	1	3.07	2
1124	2.954	7	2.941	5	2.951	6	2.937	3	2.955	10
0033	2.926	7	2.885 b	3	2.932	6	2.905	<1	2.936	7
122	2.842	13	2.833	7	2.843	13	2.828	8	2.845	13
125	2.819 b	17	2.810	12	2.814 b	17	2.806	9	2.819 b	19
217	2.792	7	2.781 b	6	2.785	8	2.777	3	2.795	6
2110	2.734	10	2.731	5	2.732	10	2.723	4	2.760	12
1211	2.710	3	2.703	4	2.704 b	3	2.695	1	2.711	6
2026	2.639	5	2.633	6	2.642 b	9	2.629	5	2.639	14
1214	2.632	15	2.622	8	2.627	9	2.615	7	2.634	19
2116	2.568	9	2.560	5	2.572	3	2.557	3	2.571	7
0228	2.538	4	2.533 b	2	2.534	2	2.529	1	2.546	6
306	2.487	4	2.475 b	2	2.477 b	2	2.470	<1	2.486 b	3
0039	—	—	—	—	—	—	—	—	—	—
0138	2.396	13	2.389	4	2.394	6	2.389	4	2.402	11
2032	2.349	5	2.343 b	3	2.349	3	2.336	1	2.350	4
0234	2.261	6	2.262 b	3	2.266	4	2.257	1	2.270	3
223	2.178	3	2.165 b	2	2.170 b	2	2.169 b	<1	2.176	4
a (Å)	8.716(2)		8.676(6)		8.688(10)		8.660(7)		8.710(6)	
c (Å)	96.08(4)		95.56(8)		96.2(1)		95.8(1)		96.4(1)	

PU 38/1 $H_{6.00}(K_{2.70}Na_{0.30})(Al_{4.62}Fe_{0.38})P_{8.00}O_{32}\cdot 18.00H_2O$
PU 71/3 $H_{5.64}(K_{2.73}Na_{0.09}Ca_{0.10})(Al_{4.75}Fe_{0.33})P_{8.05}O_{32}\cdot 18.13\,H_2O$
PU 71/4 $H_{5.56}(K_{2.86}Na_{0.07}Ca_{0.04})(Al_{4.86}Fe_{0.15})P_{8.02}O_{32}\cdot 18.62H_2O$
PU 71/6 $H_{5.16}(K_{2.44}Na_{0.26}Ca_{0.17})(Al_{4.75}Fe_{0.30})(P_{7.862}S_{0.22})O_{32}\cdot 18.69H_2O$
PU 502/2 $H_{5.51}(K_{2.67}Na_{0.15}Ca_{0.10})(Al_{4.61}Fe_{0.42})(P_{7.93}S_{0.12})O_{32}\cdot 18.89H_2O$

Note: The formulas have been calculated on the basis of 32 O atoms and 16 cations.

Å, 2.90 Å)—that we have referred to as $KAlP_2O_7$—at 1000 °C. They concluded that the reversibility of the modifications was the result of a rapid phase transformation. Our results do not confirm these observations. X-ray diffraction patterns of the samples heat treated at 1200 °C and then quenched to room temperature show that $AlPO_4$ is the predominant or the only phase present. Such discrepancies might be related to the partial loss of P. In any case, when it occurs, the transformation is not reversible.

DISCUSSION AND CONCLUSIONS

The data obtained in this study provide further information on the mineralogical properties of BR, HAP, and TR, which occur together in cave deposits. It is generally accepted that BR is formed by interaction between phosphatic solutions, derived from the breakdown of guano, and limestone. This mechanism explains the origin of the Apulian BR, present as a soft layer under the guano, where the guano is in contact with the limestone. However, the small pulverulent aggregates of BR within bat guano not in direct contact with the limestone neither have fallen from the roof of the caves nor are the result of water transport of calcitic grains because of their irregular form and distribution and the total absence of calcite in the nodules. On the basis of this depositional evidence, we suggest that BR could also be formed by a chemical reaction between a phosphatic solution and bicarbonatic H_2O.

The origin of HAP is also not known, although a transformation from BR through octacalcium phosphate has been hypothesized for human stones. A review of this topic is given by Ohta and Tsutsumi (1982). Such a hypothesis cannot explain the origin of HAP in caves because the high chemical purity of BR documented herein

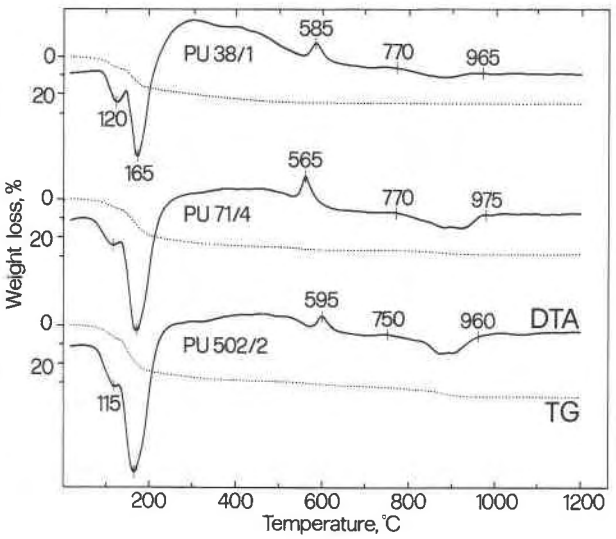

Fig. 2. DTA and TG curves of taranakite.

does not reflect the presence of foreign elements in the HAP structure. Therefore, it is likely that the precipitation of BR and HAP crystals occurs at the same time directly from solution as will be discussed later.

The mode of occurrence of TR agrees with the hypothesis that this mineral is a product of a chemical reaction between clay minerals and a phosphatic solution derived from guano. Indeed, we have observed lower contents of illite and kaolinite in "terra rossa" at the contact with TR. These clay minerals are also characterized by smaller crystallinity indices than where TR is absent. The occurrence of TR as fine layers in the guano may be because the circulation of H_2O transports significant quantities of clay minerals from "terra rossa."

The coexistence of the minerals studied gives some information about cave genetic environments. BR and HAP form in solutions having acidic and alkaline pH, respectively, and the boundary between their fields of nucleation lies in the pH range 6.2–6.8 (Simpson, 1964). Both the modes of occurrence and the larger amount of BR compared to HAP might result from a pH more favorable to the nucleation of BR. In fact, the small amounts of HAP cannot be related to the presence of a high Mg content, which can inhibit HAP nucleation (Boistelle and López-Valero, 1986), because no magnesium phosphates were found. An acidic pH is also indicated by the presence of TR because it precipitates and is stable in a highly acidic environment (Haseman et al., 1950, 1951; Filipov, 1978a, 1978b). Therefore, it is likely that the minerals studied were formed at low pH, and HAP precipitated successively only when the Ca/P molar ratio was favorable (Elliot et al., 1959; see Flicoteaux and Lucas, 1984, p. 292). Such a hypothesis might not be applicable for cave PU 1211 because TR is absent. Furthermore, taking into account that HAP is more abundant than BR and is more crystalline, it is likely that in this cave it crystallized in a neutral or a slightly alkaline environment, in which HAP is a more stable phase than BR (Posner et al., 1984).

All the elements that occur in the phosphate mineral phases we analyzed are the constituents of substratum minerals or guano; the latter contains P and also Na, K, Ca, Mg, Al, Fe, and S, as reported by Martelli (1925) and Hutchinson (1950). Only the Zn in HAP presents a problem because Zn occurs in small amounts both in the limestone and in the guano. It is unlikely that limestone is the primary source of Zn because it is necessary to hypothesize dissolution of very great quantities of limestone; in fact Moresi (1975) reports a mean value of 148 ppm for Apulian "terra rossa." Therefore, although we have detected only 500 ppm of Zn in guano, the guano remains the only identifiable source.

In summary, the chemical composition and physical properties of BR from Apulian caves are consistent with the tendency of this mineral to crystallize in very pure form. In contrast, HAP and TR show several substitutions. In HAP, Ca may be replaced by Zn, Mg, Na, and K, whereas P is replaced by S. In taranakite, Na and Ca may substitute for K, Fe for Al, and S for P. The H_2O content of TR shows slight variability and seems to increase with increasing *c*. The causes of the variations of the chemical composition of TR and HAP remain unknown.

Acknowledgments

We are grateful to L. Dell'Anna (Bari University) for the review of an early version of the manuscript. We are also indebted to J.M. Hughes (Miami University) and H.C.W. Skinner (Yale University), whose comments and suggestions have improved the paper. This study was financially supported by Consiglio Nazionale delle Ricerche.

References cited

Balenzano, F., Dell'Anna, L., and Di Pierro, M. (1974) Ricerche mineralogiche su alcuni fosfati rinvenuti nelle Grotte di Castellana (Bari): Strengite alluminifera, vivianite, taranakite, brushite e idrossiapatite. Rendiconti della Società Italiana di Mineralogia e Petrologia, 30, 543–573.

——— (1976) Francoanellite, $H_6K_3Al_5(PO_4)_8 \cdot 13H_2O$, a new mineral from the caves of Castellana, Puglia, southern Italy. Neues Jahrbuch für Mineralogie Monatschefte, 2, 49–57.

Boistelle, R., and López-Valero, I. (1986) Nucleation and growth of calcium and magnesium phosphates. In R. Rodríguez-Clemente and Y. Tardy, Eds., Proceedings International Meeting: Geochemistry of the Earth Surface and Processes of Mineral Formation, p. 811–827. CSIC, Madrid.

Deer, W.A., Howie, R.A., and Zussmann, J. (1965) Rock-forming minerals, vol. 5, p. 323–338. Longmans, London.

Elliot, J.S., Sharp, R.F., and Lewis, L. (1959) The effect of molar Ca/P ratio upon the crystallization of brushite and apatite. Journal of Physical Chemistry, 63, 725–726.

Filipov, A. (1978a) Taranakite from two deposits in Bulgaria. Annuaire de l'Universite de Sofia, 70, 287–298 (in Bulgarian).

——— (1978b) Thermodynamic analysis of the genesis of taranakite in the system $(K,NH_4)_2O$-CaO-Al_2O_3-P_2O_5-H_2O. Annuaire de l'Universite de Sofia, 70, 299–307 (in Bulgarian).

Fleischer, M. (1987) Glossary of minerals species (5th edition), 234 p. Mineralogical Record, Tucson, Arizona.

Flicoteaux, R., and Lucas, J. (1984) Weathering of phosphate minerals. In J.O. Nriagu and P.B. Moore, Eds., Phosphates minerals, p. 292–317. Springer-Verlag, Berlin.

Haseman, J.F., Brown, E.H., and Whitt, C.D. (1950) Some reaction of phosphate with clay and hydrous oxides of iron and aluminum. Soil Science, 70, 257–271.

Haseman, J.F., Lehr, J.R., and Smith, J.P. (1951) Mineralogical character of some iron and aluminum phosphates containing potassium and ammonium. Soil Science Society of America Proceedings, 15, 76–84.

Hutchinson, G.E. (1950) The biogeochemistry of vertebrate excretion. Bulletin American Museum of Natural History, 96, 275 (not seen; extracted from American Mineralogist, 37, 905, 1952).

Martelli, D. (1925) Guani. Nuova enciclopedia di chimica scientifica, tecnologica e industriale, vol. 13, p. 353–359. UTET, Turin, Italy.

McConnell, D. (1976) Hypothetical phyllophosphate structure for taranakite. American Mineralogist, 61, 329–331.

Moresi, M. (1975) Elementi in tracce di "terre rosse" pugliesi: II tenori di Zn. Periodico di Mineralogia, 44, 69–102.

Murray, J.W., and Dietrich, R.V. (1956) Brushite and taranakite from Pig Hole Cave, Giles County, Virginia. American Mineralogist, 41, 270–280.

Ohta, M., and Tsutsumi, M. (1982) The relationship between the morphology of brushite crystal grown rapidly in silica gel and its structure. Journal of Crystal Growth, 56, 652–658.

Orofino, F. (1965) Elenco delle grotte pugliesi catastate fino al 31 gennaio 1965. Rassegna Speleologica Italiana, 17, 59–81.

Posner, A.S., Blumenthal, N.C., and Betts, F. (1984) Chemistry and structure of precipitated hydroxyapatite. In J.O. Nriagu and P.B. Moore, Eds., Phosphates minerals, p. 330–350. Springer-Verlag, Berlin.

Sakae, T., and Sudo, T. (1975) Taranakite from the Onino-Iwaya limestone cave at Hiroshima Prefecture, Japan: A new occurrence. American Mineralogist, 60, 331–334.

Simpson, D.R. (1964) The nature of alkali carbonate apatites. American Mineralogist, 49, 363–376.

Smith, J.P., and Brown, W.E. (1959) X-ray studies of aluminum and iron phosphates containing potassium or ammonium. American Mineralogist, 44, 138–142.

Manuscript received August 7, 1990
Manuscript accepted May 17, 1991